



Power Performance Measurements of the NREL CART-2 Wind Turbine Using a Nacelle-Based Lidar Scanner

ANDREAS RETTENMEIER, DAVID SCHLIPF, INES WÜRTH, AND PO WEN CHENG

Stuttgart Chair of Wind Energy, University of Stuttgart, Stuttgart, Germany

(Manuscript received 26 July 2013, in final form 5 July 2014)

ABSTRACT

Different certification procedures in wind energy, such as power performance testing or load estimation, require measurements of the wind speed, which is set in relation to the electrical power output or the turbine loading. The wind shear affects the behavior of the turbine as hub heights and rotor diameters of modern wind turbines increase. Different measurement methods have been developed to take the wind shear into account. In this paper an approach is presented where the wind speed is measured from the nacelle of a wind turbine using a scanning lidar system.

The measurement campaign was performed on the two-bladed Controls Advanced Research Turbine (CART-2) at the National Wind Technology Center in Colorado. The wind speed of the turbine inflow was measured and recalculated in three different ways: using an anemometer installed on a meteorological mast, using the nacelle-based lidar scanner, and using the wind turbine itself. Here, the wind speed was recalculated from turbine data using the wind turbine as a big horizontal anemometer. Despite the small number of useful data, the correlation between this so-called rotor effective wind speed and the wind speed measured by the scanning nacelle-based lidar is high.

It could be demonstrated that a nacelle-based scanning lidar system provides accurate measurements of the wind speed converted by a wind turbine. This is a first step, and it provides evidence to support further investigations using a much more extensive dataset and refines the parameters in the measurement process.

1. Introduction

Different certification procedures in wind energy—for example, power performance testing or load estimation—require measurements of the wind speed. Nowadays, such wind speed data are usually obtained using anemometers installed on a meteorological mast. Increasing hub heights and rotor diameters also increase wind shear effects on the loading and the electrical power output of a wind turbine. One promising method of taking the shear effect into account is the use of an additional remote sensing device—for example, a sodar or a lidar system—installed on the ground as a supplement to a meteorological mast. This remote sensing device is able to measure the wind speed across the whole rotor area up to tip height and is able to take shear effects into

account (Wagner 2010). It will be used for future power performance testing on flat terrain, as this approach is fed into the revision of the current standard. Using a scanning lidar, horizontally mounted on the nacelle of a wind turbine, it is possible to gather wind speed information from a certain distance in front of a wind turbine too. The swept rotor area and shear effects of the atmospheric boundary layer are also taken into account, as is the case with a ground-based lidar system. The advantage is that this method is not only used for on-shore sites but also for offshore sites.

2. Site description

The measurement data were gathered in parallel to another campaign that mainly focused on the first field test of a lidar-assisted feedforward controller. The campaign was performed on the two-bladed Controls Advanced Research Turbine (CART-2) at the National Wind Technology Center (NWTC) in Colorado. The test site is located approximately 8 km south of Boulder and

Corresponding author address: Andreas Rettenmeier, Stuttgart Chair of Wind Energy, University of Stuttgart, Allmandring 5B, 70569 Stuttgart, Germany.
E-mail: rettenmeier@ifb.uni-stuttgart.de

consists of flat terrain with short vegetation (Clifton et al. 2013). The site comprises not only the CART-2 turbine but also three neighboring turbines and their respective meteorological masts. The sectors around the turbine, where the measurements are not influenced by other turbines or obstacles, were defined according to the current standard for power performance testing (IEC 2005).

3. Measurement setup

The CART-2 is a two-bladed wind turbine with a rotor diameter D of 42 m, a hub height of 36.6 m, and a rated power output of 660 kW, which is reached at a wind speed of around 12.6 m s^{-1} (Bossanyi et al. 2010).

The mast is located at a distance of twice the rotor diameter to the west of the CART-2 and is equipped with several sensors. The wind measurement data used in this experiment are gathered by the hub height cup anemometer only. The anemometer used has an uncertainty of $\pm 0.1 \text{ m s}^{-1}$. The overall uncertainty of the measurement chain, including cup anemometer, signal transducer, and data acquisition system, is $\pm 0.2 \text{ m s}^{-1}$.

The lidar system was installed on the nacelle of the CART-2 to measure the inflowing wind field. This means that the blades were passing the system and were blocking the laser beam. Hence, approximately 17% of the measured lidar data had to be filtered. The settings of the lidar system were mainly designed for the first field test of a lidar-assisted feedforward controller (Schlipf et al. 2012). The lidar system comprises the customary pulsed wind lidar device, “WLS7,” from Leosphere and a scanning system, specially developed at the Stuttgart Chair of Wind Energy (Rettenmeier et al. 2010). The measurement of a three-dimensional wind speed vector field by a wind lidar system (WLS) is possible because of the aerosols present in the atmosphere. In fact, these particles (dust, water, ice, pollutants, etc.) are moving with the same speed and direction as the wind. The emitted laser of the WLS is reflected by them, but it changes its frequency. This change of frequency depends on the aerosols’ speed and is based on the Doppler effect. It is only possible to measure the projection of the wind speed on the direction of the laser beam, the so-called line-of-sight velocity. For the reconstruction of the real wind speed, meaning the calculation of the three-dimensional wind vector, at least three measurement points in space are necessary. The developed laser scanner is able to steer the laser beam in any direction using a mirror. This mirror can be positioned within definite angles horizontally and vertically, and the laser beam follows a prescribed path, a so-called trajectory. As it is a pulsed laser beam, measurements

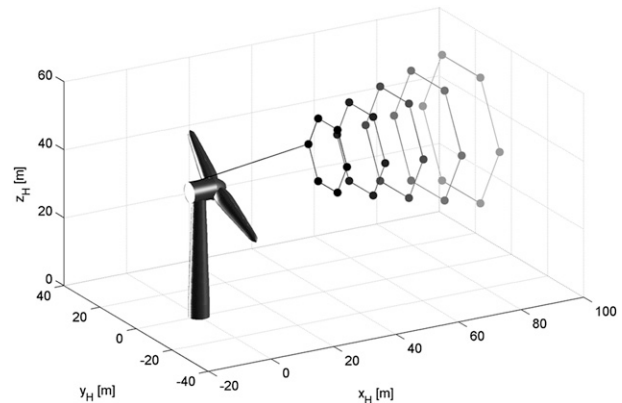


FIG. 1. Trajectory used for the CART-2 campaign. The lidar is located on top of the nacelle behind the rotor blades and is aligned with the rotor axis.

can be taken at five focus distances simultaneously. At each focus plane, a maximum of 49 discrete points can be determined, forming an arbitrary trajectory that is adapted to a certain application. Therefore, measuring with a high temporal and spatial resolution of the inflowing wind field is possible. According to the manufacturer, the uncertainty in wind speed measurement of the lidar is 0.2 m s^{-1} , assuming a carrier-to-noise ratio (CNR) higher than -18 dB over all measurement distances (Cariou 2013). In a previous measurement campaign at the wind test site of the Technical University of Denmark near Roskilde, the whole scanning lidar system was validated against a meteorological mast. The system consists of the lidar, scanner, signal transducers, and the data acquisition system. For the acquisition of a single measurement, 2000 pulses with an average duration of 0.144 s were used. For each distance, data points with bad synchronization between the lidar and the movement of the scanner or low CNR were removed. This means that data with a CNR less than -18 dB were not considered. The mast was equipped with 3D ultrasonic anemometers on one side and first-class cup anemometers on the other side of the mast boom. The configuration of the anemometers installed at three different heights allowed a precise validation of the whole measurement chain of the scanning system. During the Danish campaign, the overall uncertainty of measuring wind speed with the lidar scanner was confirmed with 0.2 m s^{-1} (Rettenmeier et al. 2012).

The trajectory and the focus distances were optimized for the controller field test at the NWTC. There was therefore no adaptation or optimization done in terms of power performance testing. Figure 1 depicts the trajectory used for the CART-2 campaign. The six measurement points at each focus plane form a hexagonal

trajectory. It takes approximately 1.3 s for one turn to measure these six points. The wind field is measured at five focus distances ranging from $1D$ to $2D$ in equidistant distances. The diameter of the inscribed circle is the same as the rotor diameter at a distance equal to $2D$.

4. Rotor effective and rotor equivalent wind speed

As mentioned before, the knowledge of the given wind speed is crucial for different wind energy applications. To describe the power performance of a wind turbine, the electrical output is set in relation to a reference wind speed. Because of the increasing rotor diameters and hub heights, the influence of the wind shear becomes an important issue with regard to power production. In Wagner (2010) the determination of an equivalent wind speed over the swept rotor disc is described. This approach takes vertical wind shear into account. For this purpose information is needed that is either provided by a meteorological mast as high as the maximum blade tip height or by an additional ground-based remote sensing device, such as a lidar. Usually, the meteorological mast reaches the height of the hub of the turbine, not higher. This is due to the mast costs and installation costs involved. Hence, the precise shear information over the swept rotor disc cannot be taken into account.

a. Rotor equivalent wind speed

Using a scanning lidar mounted on the nacelle, the whole swept rotor area can be considered. This is also the case if a ground-based profiling lidar is used. In the case of the measurement campaign described above, the six measurement points are measured at each of the five focus distances simultaneously. Two points are below, two are at hub height, and two are above hub height. This means that shear information is included in the trajectory and data.

A detailed description of a method to calculate different measurement points in time and space to a single wind speed can be found in Schlipf et al. (2013). It is hereinafter called rotor equivalent wind speed v_{0L} . With this method the lidar measures the line-of-sight velocities at the given 30 points. In the next step, the line-of-sight velocities are split into the u , v , and w wind components. The u component is aligned with the rotor axis, the v component is horizontally orientated and perpendicular to the rotor axis, and the w component is vertically orientated and is also perpendicular to the rotor axis. For this campaign it is assumed that the turbine is perfectly aligned with the prevailing wind direction and that there is no vertical wind speed. Hence, the v and w components have been set to zero. The resulting u components are averaged over a whole

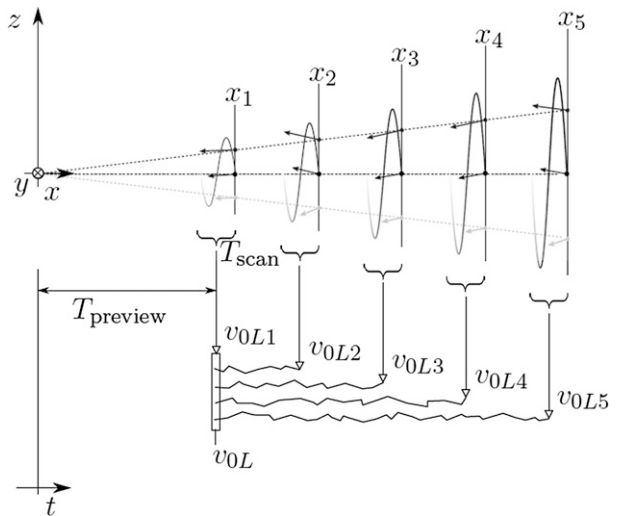


FIG. 2. Schematic drawing of the incoming wind field measured by a lidar at different focus distances x_i , and the averaged equivalent wind speed v_{0Li} at each distance.

trajectory at each focus distance. In a further step, v_{0L} is an average over all v_i available during time t (Fig. 2). That means that the five focus distances are shifted to one distance. This shift can be done with the use of Taylor's frozen turbulence hypothesis, which is valid for horizontal lidar measurements (Schlipf et al. 2010).

b. Rotor effective wind speed

The so-called rotor effective wind speed v_0 is obtained from simulated turbine data by an observer as presented in Schlipf et al. (2013). To estimate v_0 , a set of data of the aerodynamic torque of the rotor M_a , the rotor speed Ω , and the pitch angle θ is needed. A three-dimensional lookup table $v_0(M_a, \Omega, \theta)$ is generated that can then be used to get a time series of v_0 by a three-dimensional interpolation. The turbine itself thus represents a big horizontal-axis anemometer.

5. Results

a. Comparison of a high-resolution time series

In Fig. 3 the three different wind speeds are shown in a 10-min time series: one is measured by the single anemometer on the meteorological mast v_M , and the other one shows the v_{0L} measured with the lidar from the nacelle of the turbine and averaged over 30 measurement points. The third wind speed is v_0 from the turbine data. This 10-min series represents an example of the entire dataset. The v_{0L} corresponds much better to the v_0 than does the wind speed measured by the anemometer on the meteorological mast.

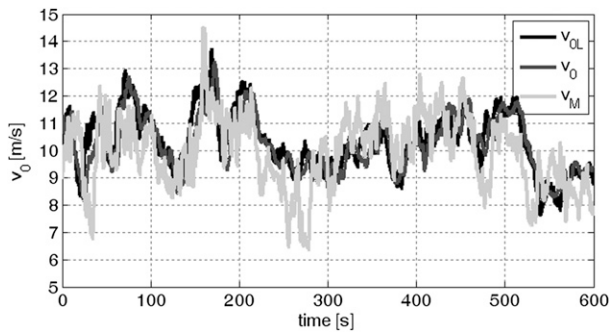


FIG. 3. Time series of the rotor equivalent wind speed from lidar (v_{0L}), of the rotor effective wind speed from turbine data (v_0) and of the anemometer mounted on a mast (v_M).

b. Correlation studies

The v_0 was set in relation to the wind speed measured by the mast-mounted anemometer v_M (Fig. 4) and in relation to the v_{0L} (Fig. 5). The data points used for the correlation studies are averaged in blocks of 30 s due to the lack of data.

A simple regression analysis was carried out. Because the model is linear with a single independent variable, the coefficient of determination (R^2) is equal to the square of the Pearson correlation coefficient r_{xy} . In statistics r_{xy} is a measure of the linear correlation and indicates the dependence between two variables. In both figures a certain offset and slope were detected that are caused by the estimation of the rotor effective wind speed. For a more precise estimation, the losses of the low-speed shaft torque should have been known. Normally, the observer has to be adapted in that way first, that the slope and the offset between rotor effective wind speed and wind speed of the meteorological mast are set to “one” or “zero” as a basis for discussion. Because of the lack of data, this was not possible.

Independent of slope and offset, it is visible that the R^2 of the correlation $v_0 - v_{0L}$ (Fig. 5) is better compared to the R^2 of the correlation $v_0 - v_M$ (Fig. 4). The following reasons could be responsible: the lidar measurements take only the u component into account, whereas the anemometer measures the u and v components of the wind speed. In the case of a yaw misalignment between the prevailing wind direction and the azimuthal orientation of the wind turbine, the coefficient of determination of the correlation $v_0 - v_M$ is lower. Because the probe volume of the pulsed lidar system the data are low-pass filtered in a certain way when measuring the wind speed. A wind turbine itself reacts to the change of wind speed in a similar way because of the mass of inertia (rotating masses such as the hub or the rotor blades). This means that there is also a kind of low-pass filtering. For this reason the correlation $v_0 - v_{0L}$ is higher.

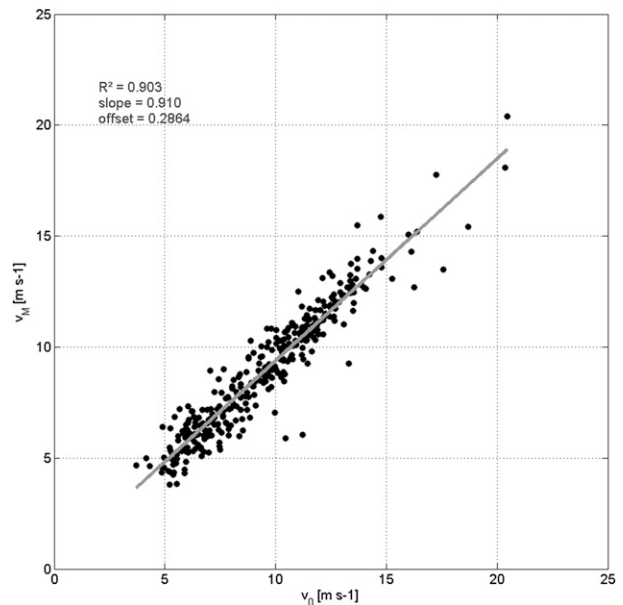


FIG. 4. Correlation between the rotor effective wind speed from turbine data (v_0) and of the anemometer mounted on a mast (v_M).

Further measurement campaigns with much more data and further investigations have to be carried out to better specify the correlation. In our point of view, the lidar measurements represents much better the prevailing wind regime, which is converted by the turbine from flow energy and mechanical energy into electrical power.

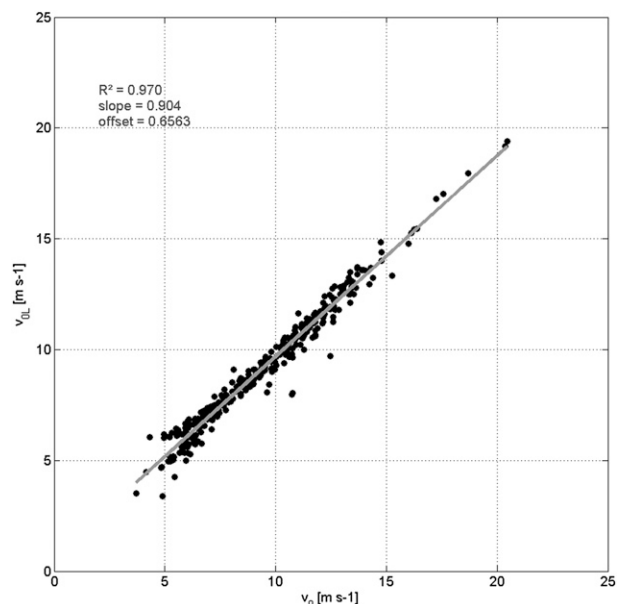


FIG. 5. Correlation between the rotor effective wind speed from turbine data (v_0) and the rotor equivalent wind speed from lidar (v_{0L}).

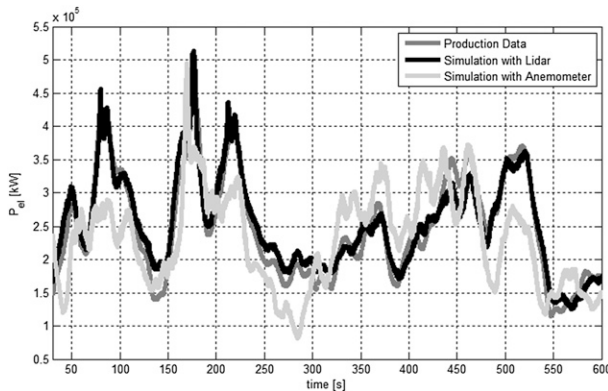


FIG. 6. Comparison of the real power output with simulated power production using wind speed data of the meteorological mast and the lidar.

c. Power performance simulation

The power production of the CART-2 turbine was simulated with the computer-aided engineering tool “FAST,” which is a software program for nonlinear aeroservoelastic analysis of horizontal-axis wind turbines. The simulation code enables prediction of wind turbine loads and responses (Jonkman and Buhl 2005). As input for a power performance simulation, a model of the turbine is needed. The model consists of the definition of sizes, masses, drag and lift coefficients, airfoils, and the controller. Furthermore, a generic wind field or wind speed data are needed. Regarding the wind speed, two different datasets were used in the simulation: v_M and v_{0L} . In Fig. 6 the result of the simulated power output is shown together with the real electrical power from the turbine. As one can see, the simulation with the rotor equivalent wind speed corresponds very well to the real production data of the turbine.

6. Summary and outlook

The measurement data gathered during the first field test of a lidar-assisted feedforward controller was investigated in terms of power performance behavior. The rotor effective wind speed, which is recalculated from turbine data, was compared to the rotor equivalent wind speed measured by a scanning nacelle lidar and the wind speed measured by a mast-mounted anemometer. The correlation between the rotor effective wind speed and the rotor equivalent wind speed is higher.

During this CART-2 campaign, the wind conditions were not optimal and therefore insufficient data were gathered to fill the required wind speed bins required by the current standard for power performance measurements. The promising results should lead to further

measurement campaigns that specially focus on power performance measurements. Furthermore, a ground-based lidar could be installed in addition to the meteorological mast aiming to gather information on wind speed at greater heights than the mast and across the rotor disc.

When transferring this approach to other turbine sizes and other rotor diameters, further investigations are necessary regarding the design of the trajectory and the relevant focus distances in front of the turbine. Hence, it could make sense to build up a simulation environment with a numerical wind field simulation, an aeroelastic wind turbine simulation, and a lidar simulation. This would lead to an optimization of the flexible parameters as well as the numbers and positions of the measurement points of the nacelle lidar.

Acknowledgments. This work was performed at NREL’s National Wind Technology Center (NWTC), Colorado. The authors thank everyone involved in getting the lidar system and the different measurement campaigns working. Special thanks to the additional members of the SWE-Lidar Group of the University of Stuttgart: Jan Anger, Martin Hofsäb, Florian Haizmann, and Oliver Bischoff as well as Alan Wright, Paul Fleming, Andrew Scholbrock, and Paul Veers from NREL.

REFERENCES

- Bossanyi, E., A. Wright, and P. Fleming, 2010: Controller field tests on the NREL CART2 turbine. NREL Tech. Rep. NREL/TP-5000-49085, 43 pp. [Available online at <http://www.nrel.gov/docs/fy11osti/49085.pdf>.]
- Cariou J.-P., 2013: Pulsed lidars. Remote sensing for wind energy, DTU Wind Energy E-Rep. DTU Wind Energy-E-Report-0029(EN), 104–121.
- Clifton, A., S. Schreck, G. Scott, N. Kelley, and J. K. Lundquist, 2013: Turbine inflow characterization at the National Wind Technology Center. *J. Sol. Energy Eng.*, **135**, 031017, doi:10.1115/1.4024068.
- IEC, 2005: Annex A: Assessment of obstacles at the test site. Wind turbines—Part 12-1: Power performance measurements of electricity producing wind turbines. 1st ed., IEC 61400-12-1, International Electrical Commission, 33–35.
- Jonkman, J. M., and M. L. Buhl Jr., 2005: FAST user’s guide. NREL Tech. Rep. NREL/EL-500-38230, 125 pp.
- Rettenmeier, A., O. Bischoff, M. Hofsäb, D. Schlipf, and J. J. Trujillo, 2010: Wind field analyses using a nacelle-based LiDAR system. *Proc. 2010 European Wind Energy Conf. and Exhibition*, Warsaw, Poland, EWEA, 416. [Available online at http://proceedings.ewea.org/ewec2010/allfiles/416_EWEC2010presentation.ppt.]
- , and Coauthors, 2012: Turbulence and wind speed investigations using a nacelle-based lidar scanner and a meteorological mast. *Proc. 2012 European Wind Energy Conf. and Exhibition*, Copenhagen, Denmark, EWEA, 883. [Available online at <http://www.ewea.org/annual2012/conference/proceedings/>.]

- Schlipf, D., and Coauthors, 2010: Testing of frozen turbulence hypothesis for wind turbine applications with a scanning LIDAR system. *15th Int. Symp. for the Advancement of Boundary Layer Remote Sensing*, Paris, France, ISARS, 4 pp. [Available online at <http://elib.uni-stuttgart.de/opus/volltexte/2013/8587/>.]
- , P. Fleming, F. Haizmann, A. Scholbrock, M. Hofsäß, A. Wright, and P. W. Cheng, 2012: Field testing of feedforward collective pitch control on the CART2 using a nacelle-based lidar scanner. Preprints, *The Science of Making Torque from Wind*, Oldenburg, Germany, EWEA, 10 pp. [Available online at <http://elib.uni-stuttgart.de/opus/volltexte/2013/8518/>.]
- , D. J. Schlipf, and M. Kühn, 2013: Nonlinear model predictive control of wind turbines using LIDAR. *Wind Energy*, **16**, 1107–1129, doi:10.1002/we.1533.
- Wagner, R., 2010: Accounting for the speed shear in wind turbine power performance measurement. Ph.D. thesis, Risø National Laboratory for Sustainable Energy, Risø-PhD-58 (EN), 124 pp.